Empirical and Analytical Determination of the Fracture Resistance of a TiB_2 Particle/SiC Matrix Composite

Michael G. Jenkins
Oak Ridge National Laboratory,* Oak Ridge, TN

CONF-891116--1

DE89 012331

Minoru Taya and Albert S. Kobayashi
Mechanical Eng. Dept.
University of Washington
Seattle, WA

Jonathan A. Salem
NASA Lewis Research Center
Cleveland, OH

*Operated by Martin Marietta Energy Systems, Inc., under contract DE-AC05-84OR21400 with the U.S. Department of Energy.

EMPIRICAL AND ANALYTICAL DETERMINATION OF THE FRACTURE RESISTANCE OF A TiB_2 PARTICLE/SiC MATRIX COMPOSITE

Michael G. Jenkins
Oak Ridge National Laboratory, Oak Ridge, TN USA
Minoru Taya and Albert S. Kobayashi
University of Washington, Seattle, WA USA
Jonathan Salem
NASA Lewis Research Center, Cleveland, OH USA

Abstract

The addition of TiB_2 particles to an SiC matrix improves machinability and the room temperature fracture resistance of the composite. Empirical tests have revealed, that the fracture resistance of this composite is a function of both loading condition (monotonic or cyclic-type) and temperature (20^oC to 1400^oC) with some dependence on specimen geometry (DCB or CNFB).

Both K_{IC} and the levels of the flat R-curves decrease with increasing temperature and are dependent on the loading condition. Fractography shows that 'toughening' contributions include particle size effects, micro-cracking at the particle/matrix interface, and crack deflection. Analytical modeling based on the residual stresses within the material due to the thermal mismatch between the particle and matrix materials compares well with the empirical results.

1. INTRODUCTION

The fracture resistance of structural materials may be quantified in a variety of ways. The methods include the fracture toughness, (K_{IC}), at crack initiation or the crack growth resistance, R-curve, during stable crack growth. Since the noteworthy work on R-curve behavior in polycrystalline alumina by Hubner and Jillek[1] over a decade ago, interest has been increasing in the use of the R-curve for more clearly characterizing the fracture resistance of ceramic materials.

In some ceramics, the observed R-curve which results from fracture resistance mechanisms may be dependent on how the loading methods affect the opening and closing of the crack faces. Similarly, those fracture mechanisms which are temperature dependent will be influenced by the testing environment and are thus reflected in the R-curve results.

Empirical fracture resistance results are presented for a commercial 16 vol% TiB_2/SiC matrix composite* under two types of loading methods (i.e. monotonic and cyclic) and at elevated temperatures (20^oC-1400^oC). Analytical modeling is conducted which relates the fracture resistance to the residual stresses.

---

*Hexoloy ST, Carborundum Company, Niagara Falls, New York

2. SPECIMEN TYPES AND MATERIAL

Two types of specimens were employed in two separate investigations for different purposes. (See Figure 1.) The chevron-notched, three-point flexure bar (CV-TPFB) was chosen for use during elevated temperature tests[2] because of the simplicity of loading and the automatic crack initiation and inherent crack growth stability afforded by the chevron notch.

The chevron-notched, wedge-loaded, double-cantilevered-beam specimen (CV-WL-DCB) was used to facilitate the evaluation of the fracture process zone using moire' interferometry at room temperature[3]. This specimen provides a large area for the diffraction grating and is also inherently stable both for crack initiation and subsequent crack growth.

Table 1 lists the specifics for the commercial, 16 vol% TiB_2/SiC material* with average particle diameter of 5 micron. This material can easily be machined using EDM methods[4,5] and it has shown enhanced fracture characteristics over the monolithic SiC matrix[2,3,6].

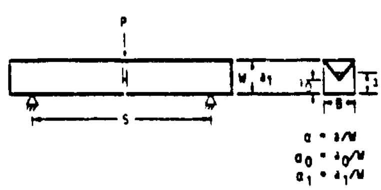

a) CV-TPFB

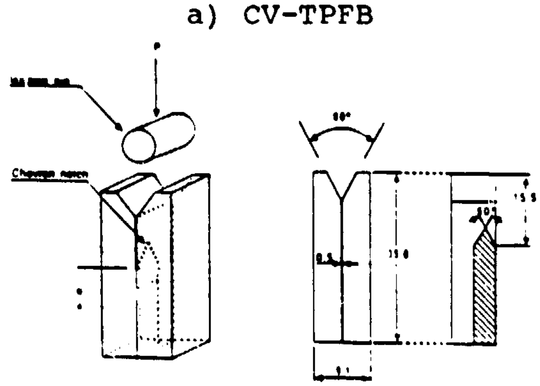

b) CV-WL-DCB

Figure 1. Specimen types.

Table I
Mechanical Properties of TiB_2/SiC Composite*

Property	Value
Elastic Modulus at R.T. (GPa)	427
Poisson Ratio	0.15
Density (kg/m^3)	3300
Flexural Strength (MPa)	448
Thermal Expansion Coefficient ($mm/mm^{o}C$)	4.2×10^{-6}
Volume Fraction of TiB_2 (%)	16
SiC matrix	alpha phase

* As given by manufacturer

3. LOADING METHODS AND RESULTS

The CV-TPFB specimens were loaded monotonically under displacement control, with no load interruptions during stable crack growth to the completion of the test (i.e. specimen fracture). Linear-elastic unloading to zero was assumed in applying the compliance method to determine the effective crack length.

The CV-WL-DCB specimens were subjected to a cyclic-type of loading with repeated load applications and reversals, under displacement control, during stable crack growth until the end of the test. The load reversals allowed the determination of the average specimen compliance and subsequently the effective crack length[7], and also facilitated the evaluation of the fracture process zone using the moire' techniques[3]. A schematic comparison of the loading methods is shown in Figure 2.

The R-curves were determined from the compliance relations for each specimen type and the loading curves for each test, using an energy method[8] shown schematically in Figure 3. The room temperature R-curves as shown in Figure 4, are flat and constant for all the specimen types and the loading methods indicating linear elastic fracture behaviour. Similar R-curves ($\approx 40\ J/m^2$) exist for the monotonically loaded CV-TPFB and CV-WL-DCB specimens. However, the R-curve for the

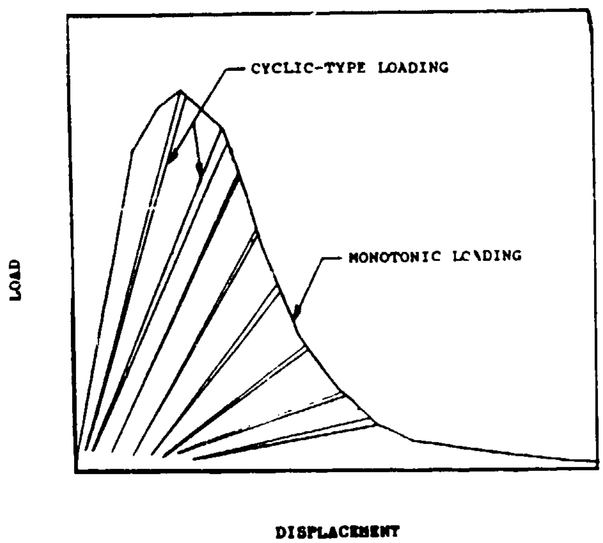

Figure 2. Loading methods.

cyclically loaded CV-WL-DCB specimens is at a lower (≈30 J/m^2) level.

Included in Figure 4 is the flat R-curve for CV-WL-DCB specimens regardless of loading method, for a similar 16 vol% TiB_2/SiC with an average particle size of about one micrometre. The level of this R-curve (≈15 J/m^2) is approximately the same as that observed for the monolithic SiC matrix[9].

Fractographic comparisons of the two loading methods did not reveal large differences indicating that the different levels of the R-curves may be related to bulk fracture effects rather than local (i.e. crack tip) effects.

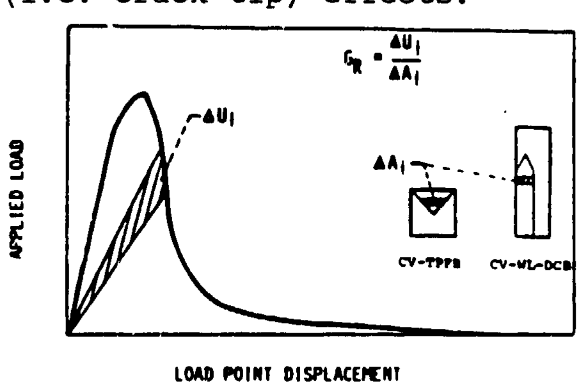

Figure 3. R-curve calculation.

4. TEMPERATURE EFFECTS AND RESULTS

The CV-TPFB specimens were fracture tested over the temperature range of 20°C to 1400°C in ambient air and relative humidity under monotonic loading. The crack mouth opening displacement was determined for the entire test using a non-contacting laser interferometric displacement gage.[2]

The critical stress intensity factor, K_{IC} as a function of temperature is shown in Figure 5. The resulting flat and constant R-curves as functions of temperature are shown in Figure 6. Although the magnitudes of the curves decrease with increasing temperature the slopes remain constant.

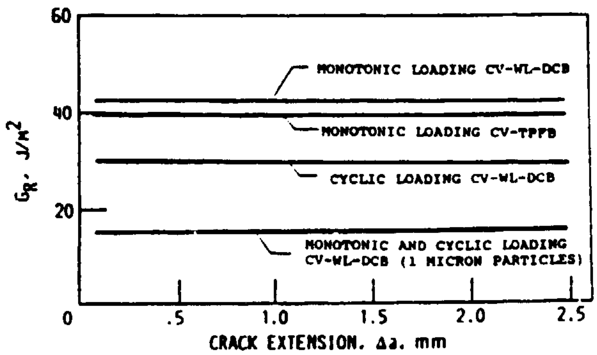

Figure 4. R-curves for loading methods.

Fractography[2] has shown that the 20°C fracture surfaces consist of ridges and valleys while the 1400°C surfaces are relatively flat and undeformed. At 20°C, crack extension occurs by linking groups of TiB_2 particles due to residual stresses, thus causing deviations in the crack path. At higher temperatures, the thermally induced residual stresses around the particles are relieved thus decreasing the fracture resistance with increasing temperature.[2]

5. ANALYTICAL MODELING

The fracture model can be thought of as a 'system' fracture resistance, G_{RS}, such that:

$$G_{RS} = G_{RC} + \Delta G \qquad (1)$$

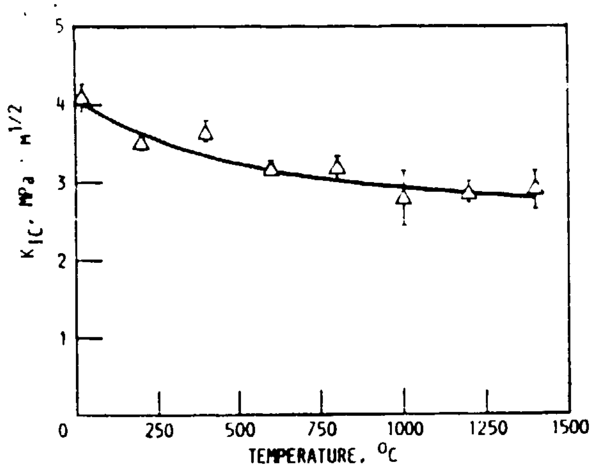

Figure 5. K_{IC} vs. temperature.

where G_{RC} is the fracture resistance of the composite constituents and ΔG is the 'toughening' component. In this study:

$$\Delta G = f\ (\sigma_{RES}) \qquad (2)$$

where σ_{RES} may represent any residual stress field in either the particle or the matrix.

G_{RC} is calculated as 15.24 J/m^2 from the rule of mixtures the relation of $G_{IC} = 2\gamma_f$ such that:

$$G_{RC} = (1-V_P)\ 2\gamma_M + (V_P)\ 2\gamma_P \qquad (3)$$

where G_{IC} is the critical strain energy release rate, γ_f is the fracture surface energy, V_P is the volume fraction of particles (subscripts M and P refer to matrix and particle, respectively) $\gamma_M \approx 6.5\ J/m^2$ for this SiC[8], and $\gamma_P \approx 13.5\ J/m^2$)[10].

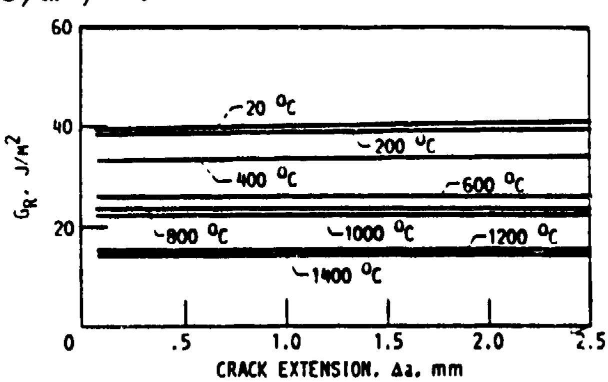

Figure 6. R-curves for temperatures.

The magnitude of ΔG at the various temperatures is shown in Table II assuming G_{RC} remains constant. Also shown in the table are the values of the calculated[11] residual stress components for a single particle in a matrix, as shown in Figure 7, using the properties in Table III.

ΔG can be written in as a strain release rate such that:

$$\Delta G = G = \Delta U/\Delta A \qquad (4)$$

where ΔU is the change in strain energy and ΔA is the area of the incremental crack extension.

The analysis of Lange[11] is used in which the stored energy associated with a particle is given as:

$$U_P = 2\ \pi\ k\ \sigma_t^{\ 2}\ R^3 \qquad (5)$$

where R is the radius of the particle and k is the constant related to the thermal mismatch.[12]

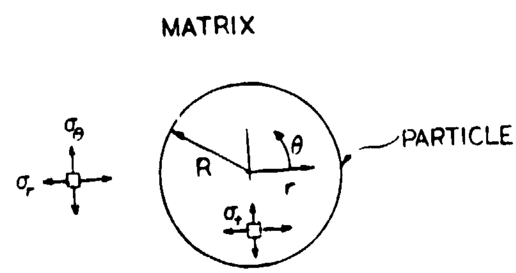

Figure 7. Components of residual stress.

A log/log plot of ΔG versus σ_t is shown in Figure 8. The slope of the line (2.2) is in good agreement with the expected slope of 2.

A linear relation exists for the 'toughening' increment, ΔG, as a function of the particle strain energy per unit area, U_P/A, as shown in Figure 9. In this case U_P/A is of the form:

$$U_P/A = \frac{N_P\ (2\pi\ k\ \sigma_t^{\ 2}\ R)}{(4(1-V_P)/3V_P)} \qquad (6)$$

where N_P is the number of particles in the unit area,

Table II
Fracture Resistance Increment and Residual Stresses for 2.5 micrometre radius particles

T [ΔT]* ($^\circ$C)	ΔG (J/m^2)	Maximum $\sigma_t = \sigma_r$ (MPa)	Minimum σ_θ (MPa)
20 [1980]	26.7	270	-135
200 [1800]	25.2	246	-123
400 [1600]	18.5	218	-109
600 [1400]	10.7	191	- 96
800 [1200]	7.6	164	- 82
1000 [1000]	6.7	136	- 68
1200 [800]	0	109	- 55
1400 [600]	0	82	- 41

* $\Delta T = T_i - T_f$ where $T_i = 2000^\circ C$, (sintering)
T_f = test temperature

Table III
Mechanical Properties* Used in Stress Calculations

Property	TiB_2 Particle	SiC Matrix
Elastic Modulus (GPa)	531	410
Poisson Ratio	0.11	0.22
Thermal Expansion Coefficient (mm/mm$^\circ$C)	4.6×10^{-6}	4.2×10^{-6}

*Assumed to remain constant for all temperatures.

thus showing that for any residual strain energy situation due to the presence of the particles, the toughening increment can be determined following the argument of Lange[12] in regard to the existence of a proportionality constant for σ_t^2 and R.

Crack deflection may not be the only 'toughening' mechanism as evidenced by the influence of cyclic loading as shown in Figure 4. Previous fractography[2] has shown, microcracking of the matrix and/or matrix/particle interfaces may relieve some of the residual stresses during the loading and unloading sequences. Thus, the fracture resistance benefits of the residual stress fields may be reduced during the subsequent stable crack growth.

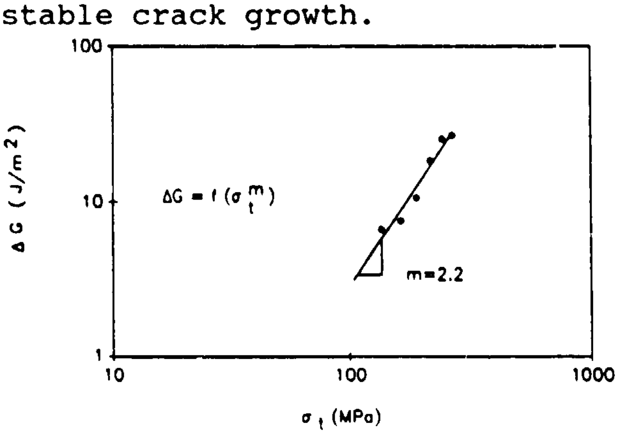

Figure 8. ΔG vs. σ_t (σ_r).

6. DISCUSSION AND CONCLUSIONS

Note the role of loading method whereby this material would be more susceptible to catastrophic failures in design applications with a cyclic type of loading, while a steady-state type of loading would produce a similar failure but at higher loads. The temperature dependence of the the fracture resistance is of particular note if this composite is to be used at elevated temperatures.

Although the R-curves in all cases should be viewed as flat and thus describing brittle, linear elastic behavior, the fracture resistance of this composite is usually greater than that of the monolithic SiC matrix. The limited analytical modeling points to the importance of the residual stress state in increasing the fracture resistance of this material. Important variables include the particle size and shape, the particle volume fraction , and the mismatches of the thermal expansion coefficients, the elastic moduli, and the Poisson ratios. Micro-cracking, while not a dominant 'toughening' mechanism, may also affect the crack deflection mechanism by relieving some of the residual stress fields, especially for a cyclic type of loading.

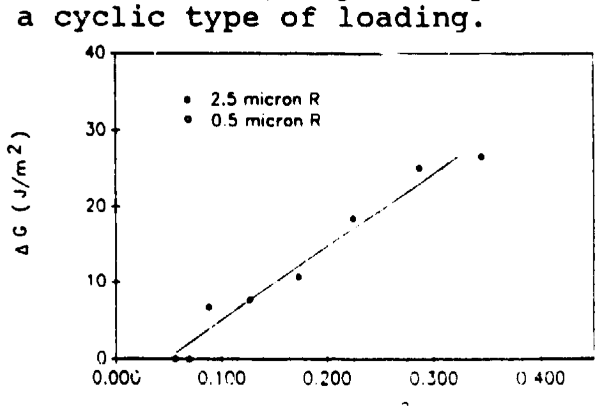

Figure 9. ΔG vs. U_p/A.

In conclusion: 1) At room temperature this SiC/TiB_2 composite shows 'toughened' fracture resistance compared to the monolithic SiC matrix, 2) A cyclic loading condition in this material during stable crack growth produces flat R-curves at levels lower than those flat R-curves observed under monotonic loading, 3) Increasing temperature decreases the levels of the flat R-curves as the 'toughening' benefits of the residual stresses around the TiB_2 particles are reduced, 4) Particulate-reinforced composites can show increased fracture resistance even for tensile-residually-stressed particles due to crack deflection caused by the residual stress field interactions.

REFERENCES

[1] H. Hubner, W. Jillek, J. Mat. Sc. 12, 117-125, (1977).
[2] M.G. Jenkins, J.A. Salem, S.G. Seshadri, J. Comp. Mat., 23, 1, 77-91, (1989).
[3] S. Hayashi, L. Deobald, M. Taya, A.S. Kobayashi, Mechanics of Composite Materials-1988, ASME AD New York, (1988).
[4] J.E. Garnier, W.D.G. Boecker, C.H. McMurty, S. Calandra, Paper No 150-C-87, 89th Annual Meeting of the American Ceramic Society (1987).
[5] S.G. Seshadri, J.E. Garnier, K.Y. Chia, Paper No 149-C-87, ibid.
[6] C.H. McMurty, W.D.G. Boecker, S.G., Seshadri, J.S. Fanghi, J.S., Am. Cer. Soc. Bul. 66, 22, 325-329, (1987).
[7] American Society for Testing and Materials, ASTM E 561-81, (1983).
[8] M.G. Jenkins, Ceramic Crack Growth Resistance Determination Utilizing Laser Interferometry, PhD Dissertation, Univ. of Wash., June 1987.
[9] A. Ghosn, M.G. Jenkins, K.W. White, A.S. Kobayashi, R.C. Bradt, J. Am. Cer. Soc., 72, 2, 242-247 (1989).
[10] M.K. Ferber, P.F. Becher, C.B. Finch, J. Am. Cer. Soc. 66, 1, C2-C4, (1983).
[11] J. Selsing, J. Am. Cer. Soc. 44, 419, (1961).
[12] F.F. Lange, in Fracture Mechanics of Ceramics, Volume 2, R.C. Bradt, A.G. Evans, D.P.H. Hasselman, F.F. Lange, Eds, Plenum Press, New York 1974, pp 599-609